

Performance Analysis of an Enhanced Spread Spectrum Aloha System

Florian Collard^{1,2}, Annamaria Recchia¹, Natalia Antip¹,
Antonio Arcidiacono¹, Daniele Finocchiaro¹, and Orazio Pulvirenti¹

¹ Eutelsat S.A., 70 rue Balard, 75502 Paris Cedex 15, France
{fcollard,arecchia,nantip,aarcidiacono,
dfinocchiaro,opulvirenti}@eutelsat.fr

² ISAE Campus Supaero, 10 Avenue Edouard Belin, 31055 Toulouse, France

Abstract. In this paper we present tests results of the first platform implementing a high performance Random Access protocol dubbed Enhanced Spread Spectrum Aloha (E-SSA), conceived for satellite applications. The aim of the study is to highlight key features of the system, introducing experimentally-found threshold values and translating them into operating conditions. A system overview is provided together with a summary of the most relevant parameters and the framework of the tests. The preamble detection and the packet demodulation processes are analysed, showing the importance of exploiting Successive Interference Cancellation techniques (SIC). It is shown that the code collision, due to a robust rate in the turbo-code and to the iterative cancellations, does not affect the system performances. Finally, Packet Loss Ratio (PLR) in presence of received carrier power and frequency unbalance is detailed with the aim of simulating more realistic scenarios.

Keywords: Random Access, Enhanced Spread Spectrum Aloha, Successive Interference Cancellation, Satellite Messaging Protocol.

1 Introduction

The launch of W2A in April 2009, carrying into orbit the first commercial S-band payload over Europe, represents a great opportunity for space telecommunications industry, given its innovative nature in the satellite domain. The MSS S-band frequencies, residing in the 2GHz band adjacent to 3G UMTS, allow the use of small omni-directional antennas and enable the deployment of satellite/terrestrial hybrid networks. Furthermore, the large reflector on-board requires a moderate EIRP at the terminal side, thus opening the way for a full exploitation of the return link (terminal-to-satellite) [1].

The S-band frequencies are well suited to the so-called intelligent devices, whose forthcoming exponential growth in the automotive and domotics worlds will benefit from a low-cost high efficient system for non-real-time communications, mainly based on messaging [2]. Telemetry, environment and traffic monitoring, emergency alerts, fleet management, highway tolling, forecast predictions,

pay-per-view represent just few among all possible applications. Road-safety and emergency applications will be tested in a real scenario through a demonstration platform built-up by SafeTRIP, a collaborative project in the framework of the EU Seventh Framework Program [3].

After a preliminary phase of system definition and performances assessment, carried-out in ESA cofunded projects MiReSys and DENISE, the Enhanced Spread Spectrum Aloha [4] has been chosen as the reference protocol for the return link physical layer specifications, with asynchronous access, and has been recently standardised at ETSI as *Air Interface for S-band Mobile Interactive Multimedia* (S-MIM), Part 3 [5]. The E-SSA structure, based on fully asynchronous random access with a robust Forward Error Correction (FEC) and a simple open loop power control, perfectly copes with low-duty cycle bursty transmission, adapted to satellite messaging. Furthermore, the introduction of ad-hoc Successive Interference Cancellation (SIC) techniques, coupled with a smart reuse of a unique hierarchic preamble, shared by the entire population of terminals, shows good results in terms of MAC throughput. The system capacity allows the simultaneous coexistence of millions of terminals in limited portions of bandwidth, thus lowering the exploitation cost per final user.

This paper presents experimental results based on the first available prototype implementing E-SSA protocol. In Section 2 a system overview is reported, focusing on system parameters. In Section 3 prominent relevance is given to the features emerging from the practical implementation of the protocol, such as the reduced impact of code collision. System capacity results, in terms of maximum allowed MAC-Loads and PLR, are then presented, through different scenarios at increasing standard deviation values in received power and at increasing uniformly distributed frequency errors.

2 System Overview

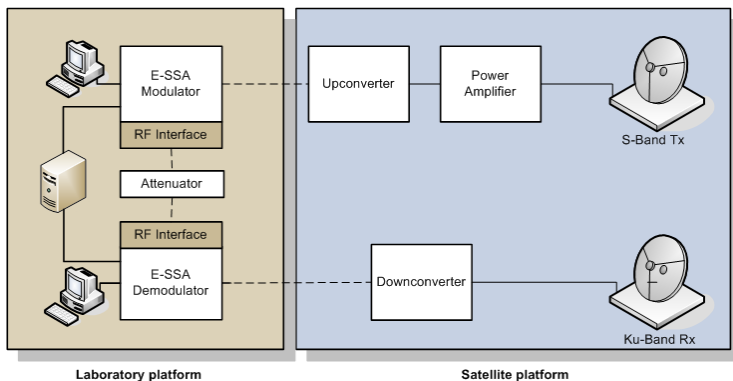


Fig. 1. E-SSA platform at Eutelsat premises

The deployed E-SSA prototype, hosted at Eutelsat premises, is tautly shown in Fig.1. It includes a traffic generator, able to simulate an aggregated signal coming from thousands of terminals simultaneously transmitting over an AWGN channel, and the first available prototype of E-SSA demodulator. Both traffic emulator and demodulator are based on Software Defined Radio (SDR) and are fully reconfigurable to work in a frequency range of 50-2200 MHz. In the present study, the experiences have been run on digital samples generated at the modulator side, stored on disk and then analysed by the demodulator (not in real-time), bypassing the radiofrequency interfaces.

Apart from the laboratory testbed, a complete satellite chain is available at Rambouillet teleport to transmit in S-band towards W2A. First on-air tests have been successfully conducted and preliminary results confirm theoretical expectations. They will constitute the basis of future work.

In Table 1, the most relevant implementation parameters, in line with the S-MIM standard [5], are reported. One of the main differences in system choices, with respect to ESA proposal [6], resides in the increased packet length of 1200 information bits, enabling an increased turbo code efficiency and minimizing the code collision. However, the extended length exposes the packet to channel variations effects within its duration, that may result in additional difficulties at phase and frequency estimation stages.

Table 1. E-SSA implementation parameters

<i>Equipment</i>	<i>Parameters</i>	<i>Value</i>
Modulator	Bandwidth	4,68 MHz
	Chip-rate	3,84 Mcps
	Spreading factor	256
	Number of spreading codes	1
	Info bits per packet	1200
	Coded bits per packet	3600
	Preamble length	96 bits
	CRC length	16 bits
	Oversampling factor	4
Demodulator	Number of SIC iterations	scalable [0-100]
	Max. demodulation attempts	800 packets/s
	Turbo codes iterations	6

Compared to the ideally-continuous packet-by-packet estimation-regeneration-cancellation process envisaged in [6], the SIC mechanism in the analysed implementation applies per groups of detected packets. The amount of packets per group can be scaled at will, defining the maximal number of possible demodulations at each interference cancellation cycle. The SIC mechanism relies on few fundamental operations carried out on each packet. Initially, the preamble searcher allows the detection of the packet. During this stage the chip-timing recovery and the frequency estimation are performed. Afterwards the packet enters its true demodulation stage. The most critical operations are the phase and

power estimations. They are performed using a channel estimator that divides each packet in slices and estimates the power and phase of each slice. From this point on, the packet is decoded and CRC checked. If the packet is judged to be correctly demodulated, it is integrated with the rest of the demodulated packets. Considering the previously recovered parameters (chip time, frequency, phase and power), the resulting stream is regenerated and subtracted from the original signal. Thanks to the previous operations, the total interference diminishes and other packets with smaller SNIR arise and are detected by the preamble detector at the following iteration. Fig. 2 well illustrates the iterative SIC behaviour.

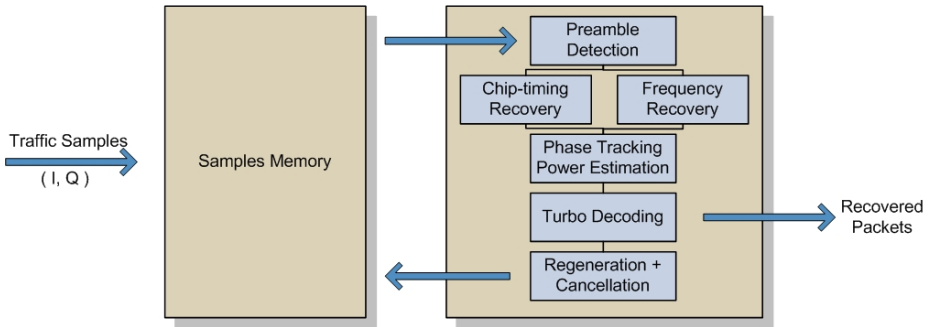


Fig. 2. Successive Interference Cancellation process

3 Performance Analysis

Experimental results coming from the E-SSA implementation allow refining the description of the demodulation process and a better understanding of its crucial steps, i.e. detection, demodulation, channel estimation and cancellation. Thanks to the use of a specific hierarchic preamble of 96 bits, whose choice has been widely motivated in [7], packet detection algorithm can work at increased MAC-Loads. For instance, at 1.28 bits/s/Hz (which correspond to 5000 packets/s, with an occupied bandwidth of 4.68 MHz and a packet length of 1200 information bits), the average E_c/N_t is equal to 30.8 dB. After the preamble correlation phase, the SNIR of the preamble can be calculated:

$$SNIR_{preamble} = \left[\frac{E_c}{N_t} \right]_{th} + 10 \log(L) + 10 \log(SF) = 13.1 \text{ dB} \quad (1)$$

where L is the preamble length in bits equal to 96 and SF is the spreading factor equal to 256, resulting to be a good value for packet detection and SIC effectiveness.

The efficiency of the turbo codes, with the choice of a robust rate ($r=1/3$) results in a lower E_b/N_t threshold for the demodulation, ensuring excellent PLR even at very low packet SNR. Keeping unvaried the assumption made in [6], i.e. packets log-normally distributed in power with a standard deviation of 3 dB, the

Table 2. PLR floors at different burst SNR

Burst SNR _{average} (dB)	PLR floor
-16	$1.3 \cdot 10^{-4}$
-17	$5.1 \cdot 10^{-4}$
-18	$1.4 \cdot 10^{-3}$
-19	$3.8 \cdot 10^{-3}$
-20	$8.7 \cdot 10^{-3}$
-21	$1.7 \cdot 10^{-2}$

system PLR floor may be evaluated. In Table 2, the good PLR values, even at very low SNR, show the system robustness in noisy environments.

Regarding the cancellation process, due to the fact that the efficiency of each stage affects the successive, it is very important to avoid to introduce residual power coming from erroneous cancellations.

The PLR can be also studied at varying MAC-Loads. In order to strictly evaluate the interference cancellation process, no noise was added, resulting in a high SNR. Results in Table 3 confirm the validity of the implemented cancellation process by group of packets.

Table 3. PLR floors for different MAC-Loads

MAC-Load (b/s/Hz)	PLR floor
0.5	$5.8 \cdot 10^{-6}$
0.7	$7.7 \cdot 10^{-5}$
1	$4.1 \cdot 10^{-4}$
1.2	$1.1 \cdot 10^{-3}$
1.5	$2.7 \cdot 10^{-3}$
1.8	$5.5 \cdot 10^{-3}$

3.1 Code Collision

The code collision corresponds to the reception of two or more packets at the gateway demodulator within a preamble detection interval. One can think that the perfect superimposition of packets makes the demodulation unfeasible. An interesting behaviour has been found out during laboratory testing of E-SSA prototype, i.e. the PLR is not lower-bounded by the code collision effect. This is mainly due to the robust rate of the turbo code and to the presence of the SIC. In fact, most of the time the two superimposed packets can be correctly demodulated, even if they have been transmitted at the same chip time. In good channel estimation conditions, if the packets have different amplitudes, it is possible to demodulate and cancel the most powerful of them at a first SIC iteration, then the second one can be found by the preamble searcher at a successive iteration. Similarly, frequency or phase differences can be useful to differentiate between two packets starting at the same time. Moreover, even if

Table 4. Code collision experimental results

MAC-Load (packets/s)	Expected PLR	Measured PLR
1000	$4.2 \cdot 10^{-4}$	$8.3 \cdot 10^{-6}$
2000	$0.9 \cdot 10^{-3}$	$1.7 \cdot 10^{-5}$
3000	$1.4 \cdot 10^{-3}$	$1.7 \cdot 10^{-5}$
4000	$1.9 \cdot 10^{-3}$	$2.7 \cdot 10^{-5}$
5000	$2.3 \cdot 10^{-3}$	$3.8 \cdot 10^{-5}$

the received packets present almost the same parameters (power, frequency and phase), the probability of good demodulation is still not null.

The explanation comes from the structure of the E-SSA signal, which is obtained by filtering a spread and scrambled BPSK sequence of symbols. From the detection point of view, receiving two different packets aligned at the chip time is equivalent to have a single packet, whose preamble amplitude is doubled, consequently easing the detection. The turbo codes will lead the decoder to choose one of the two initial sequences of information bits. The Table 4 herein confirms this behaviour, showing that collision events do not lower-bound the PLR. In fact, the measured PLR is by far lower than the expected PLR (the ratio between the number of colliding packets and the number of transmitted packets).

3.2 Power Distribution

The burst distribution in received power is one of the crucial system issues. In real scenarios, due to different G/T values within a satellite beam, to the coexistence of several transmitting antennas with distinct gains and to the impairments introduced by the mobile channel, the power received at the hub, even in presence of a quite accurate open loop power control, can vary substantially. This directly affects not only the final performances of the E-SSA demodulator in terms of achievable PLR, but also the number of iterations required to reach the fixed PLR threshold. In order to simulate these effects, a Gaussian power distribution has been chosen.

At increasing standard deviation in log-normally distributed power, two distinct effects are verified from the simulations. First of all, the number of terminals with E_b/N_t lower than the demodulation threshold increases, due to the enlarged basis of Gaussian distribution. Secondly, the SIC algorithm, starting from the cancellation of packets with the best SNIR, is better suited to high power unbalance distributions. In fact, when received power is not spread, the packet detection is much less efficient and the demodulation gets worse, because the average SNR of detected packets is lower. In Fig. 3, it is interesting to notice that up to a normalized MAC-Load of 1.7 b/s/Hz, the system performances are optimized

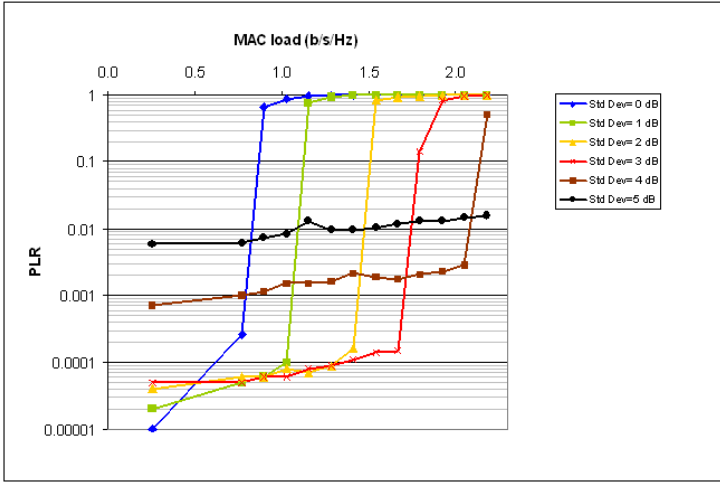


Fig. 3. PLR at increasing MAC-Loads and different values of standard deviation ($C/N = -16\text{dB}$)

at 3 dB of standard deviation both in terms of reached PLR. Above 1.7 b/s/Hz the standard deviation optimal value becomes higher.

3.3 Frequency Distribution

Several components in the E-SSA satellite transmission can introduce a frequency error: the clock instability at the terminal side, the on-board satellite frequency conversion steps, the Doppler effect due to satellite and mobile terminals, the hub frequency accuracy. While the frequency error introduced by the satellite can be compensated at the hub and the hub itself can be easily connected to a stable reference, transmitting terminals conceived for mass market distribution will not embed precise oscillators, as they are still quite expensive. Consequently, the E-SSA demodulator must manage a population of terminals having a certain frequency distribution. Henceforth, frequency errors are assumed to follow a uniform distribution.

In Fig. 4, PLR values are reported for increasing frequency errors of the aggregated traffic. From a general point of view, the demodulator behaves like a selective filter in frequency (-1.5kHz , 1.5kHz), as already demonstrated in [7].

For normalised MAC-Load values up to 1.5 b/s/Hz, the PLR is almost unvaried up to the cut-value of 1500 Hz. Above 1.5 b/s/Hz, the system performances in terms of PLR get worse at increasing frequency errors and, after 1500 Hz, the PLR increases. In other terms, above MAC-Load values of 1.5 b/s/Hz, in presence of frequency drift, the detection process becomes more difficult and higher average SNRs are required to target a fixed PLR.

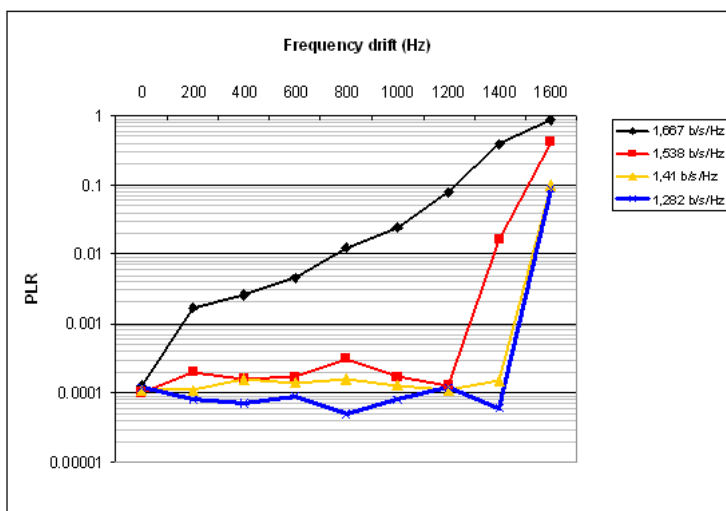


Fig. 4. PLR at increasing frequency error and fixed MAC-Loads ($C/N = -16\text{dB}$)

4 Conclusions

We have shown that the good theoretical performances of the E-SSA protocol are confirmed by a real prototype. High throughputs at very low PLR (at least 10^{-3}) have been reached and new fundamental behaviours of the system have been refined. First of all, even if the importance of received packets power unbalance in SIC mechanism had already been stated, here we have shown that to each MAC-Load corresponds an optimal value of standard deviation in the log-normally distributed received power. In an enhanced system, a simple open-loop power control mechanism could exploit this behaviour by signalling from the hub the ideal received power distribution, as foreseen in the S-MIM standard. Moreover, it has been shown that the frequency error distribution could be a constraint especially at high MAC-loads, strongly impacting the resulting PLR. Future works will deal with the introduction of a mobile channel and the assessment through the radiofrequency interfaces and the end-to-end satellite link. The channel estimation parameters will become crucial in such an environment and the impact on performances, jointly with the use of a control channel, will be studied.

References

1. Arcidiacono, A., Finocchiaro, D., Geurtz, A., Pulvirenti, O., Schluter, G.: S-band: a new age in mobile satellite systems. In: 4th Advanced Satellite Mobile Systems Conference, Bologna, pp. 122–127 (2008)
2. Arcidiacono, A., Finocchiaro, D., Grazzini, S., Pulvirenti, O.: Perspectives on mobile satellite services in S-band. In: 5th Advanced Satellite Mobile Systems Conference, Cagliari, pp. 516–521 (2010)

3. Fremont, G., Grazzini, S., Sasse, A., Beeharee, A.: The SafeTRIP project: improving road safety for passenger vehicles using 2-way satellite communications, ITS World Congress 2010, Busan (2010)
4. De Gaudenzi, R., del Río Herrero, O.: Methods, apparatuses and system for asynchronous spread-spectrum communication, European Patent 2 159 926 A1 (2010)
5. ETSI TS 102 721, Satellite Earth Stations and Systems, Air Interface for S-band Mobile Interactive Multimedia, Part 3: Physical Layer Specification, Return Link Asynchronous Access (S-MIM) (2011), <http://www.etsi.org>
6. De Gaudenzi, R., del Río Herrero, O.: Advances in Random Access Protocols for Satellite Networks. In: International Workshop on Satellite and Space Communications, Siena, pp. 331–336 (2009)
7. Demonstrator Emergency aNd Interactive S-band sErVICES (DENISE), Phase 1, Artes 3-4 Projects, Internal Reports, <http://telecom.esa.int> (2009-2011)